electronics

MDPI

Article

A Three-Phase CDRT Strategy Based on Successive Relay for Smart Grid

Mofan Luo [1], Geng Liu [2], Jie Ren [3], Liang Yao [2], Ying Liu [2], Jianjian Song [1,*], Jian Chen [1] and Yuchen Zhou [1]

[1] State Key Laboratory of Integrated Services Networks, Xidian University, Xi'an 710071, China
[2] Smart Shine Microelectronics Technology Co., Ltd., Qingdao 266317, China
[3] Beijing Smart-Chip Microelectronics Technology Co., Ltd., Beijing 100192, China
* Correspondence: m18838922338@163.com

Abstract: In the vision of the future smart grid, the communication is often featured by wide range, massive connect, and low latency, which poses new requirements on the reachable distance and spectral efficiency of wireless communication. In this regard, this paper studies ergodic capacity enhancement by applying successive relay (SR) technology to a non-orthogonal multiple access (NOMA) based Coordinated Direct and Relay transmission (CDRT) system, where a base station (BS) communicates with a near user (NU) directly while communicating with a far user (FU) with the help of a group of relays. We design a novel three-phase CDRT strategy based on SR technology to overcome the half-duplex (HD) constrain without introducing additional noise. The proposed strategy can improve the spectral efficiency while expanding the communication coverage, which to some extent improves the communication quality of the edge users of the smart grid and reduces the communication delay. To analyze the performance of the proposed three-phase CDRT strategy, an exact and closed-form expression for ergodic capacity of the NU, the FU, and the whole system is derived. Finally, the numerical and simulation results validate the analysis results and show that the proposed strategy can improve the ergodic capacity of FU without reducing the capacity scaling of NU.

Keywords: non-orthogonal multiple access; coordinated direct and relay transmission; successive relay; ergodic sum capacity

check for updates

Citation: Luo, M.; Liu, G.; Ren, J.; Yao, L.; Liu, Y.; Song, J.; Chen, J.; Zhou, Y. A Three-Phase CDRT Strategy Based on Successive Relay for Smart Grid. *Electronics* **2022**, *11*, 3673. https://doi.org/10.3390/electronics11223673

Academic Editor: Ahmed Abu-Siada

Received: 14 September 2022
Accepted: 8 November 2022
Published: 10 November 2022

Publisher's Note: MDPI stays neutral with regard to jurisdictional claims in published maps and institutional affiliations.

Copyright: © 2022 by the authors. Licensee MDPI, Basel, Switzerland. This article is an open access article distributed under the terms and conditions of the Creative Commons Attribution (CC BY) license (https://creativecommons.org/licenses/by/4.0/).

1. Introduction

With the rapid development of power equipment, the smart grid has become more automated and intelligent, which puts forward higher requirements for the communication network of the smart grid [1]. Non-orthogonal multiple access (NOMA), whose key idea is to allow multiple devices to use the same resource (time, frequency, and code) block to access the network, is a promising technique to enhance the spectral efficiency of the smart grid [2]. Among many specific techniques of NOMA, power domain NOMA has been studied by many researchers due to its wide applicability and relatively low complexity. In power domain NOMA, the receiver distinguishes different devices on the same resource block by different power levels [3]. Because of this, far and near devices are often allocated to the same resource block due to the large difference in received power. However, in many countries, the power network has a wide coverage, and the ability to resist multipoint and multiline faults is weak. Accordingly, the smart grid responsible for controlling all aspects of power business also needs a wider coverage to achieve monitoring and dispatching. In addition, a more complex plant structure is accompanied by a wider coverage, which makes long-distance communications in the smart grid often infeasible [4]. Therefore, new communication technologies and strategies are urgently needed to ensure the communication of edge users. Otherwise, the communication quality of edge users can only be guaranteed by sacrificing more energy consumption.

1.1. Related Works

Against this background, Cooperative relay has been proposed as an effective method to expand communication coverage and enhance the reliability of the network [5]. The authors in [5] applied half-duplex (HD) relays in wireless networks and develop low-complexity cooperative diversity protocols that combat fading induced by multipath propagation. The work in [6] applied a decode-and-forward (DF) relay to assist the communication of the far user (FU) in a NOMA downlink scenario where between the base station (BS) and the FU has no direct link. In the CDRT strategy proposed in this article, when the cooperative relay forwards the signal of FU, the BS can send another signal to the NU. Compared with the traditional two hop cooperative transmission strategy, the overall spectral efficiency of the system is significantly improved. To reduce the infrastructure cost, user-assisted NOMA−CDRT was investigated in [7], which utilizes idle NUs as relays to serve FUs. The work in [8] proposed a dynamic transmission scheme in user-assisted NOMA−CDRT system to improve the system reliability and the connection density. However, since HD relays can only transmit or receive signals at the same time, half of the time resources are wasted. In order to make up for the loss of time resources caused by HD relay, the authors in [9] further introduced full-duplex (FD) relays to enhance the capacity of the NOMA-based CDRT system. The research results show that although FD relay makes full use of time resources, it will lead to poor system performance in the case of high signal-to-noise ratio (SNR) due to its residual loop self-interference.

Later, successive relay (SR) technology was introduced to overcome the HD constrain [10–12], whose basic idea is to use two HD relays as transmitters and receivers alternately, so as to realize parallel transmission between the BS and the relay [13]. Research shows that SR technology can recover the multiplexing loss of HD relay network while ensuring the diversity gain [14]. However, in the SR system, the relay in the transmitting state will cause interference to the relay in the receiving state, which is called inter-relay interference (IRI) [13,15]. The work in [13] propose a SR based cooperative NOMA (SR−NOMA) system which employs amplify-and-forward (AF) relays instead of DF relays for more flexible in handling the IRI. The simulation results show that the SR−NOMA scheme achieves a lower outage probability and a higher ergodic rate than existing SR−OMA and the ideal DF FD relaying based NOMA schemes. However, AF relay will introduce additional noise, which is not the best choice to eliminate IRI. Besides, many scholars are committed to eliminating IRI through the design of precoding [16,17], but this will increase the complexity of signal encoding and decoding and may bring additional power overhead.

1.2. Motivation and Contribution

Motivated by the above observations, in this paper, we are committed to design a low complexity strategy to increase the capacity of the CDRT system without introducing additional interference. By applying SR technology to NOMA-based CDRT system, we propose a novel three-phase CDRT strategy, abbreviated as 3−CDRT. Different from the above strategy of using AF relay and precoding to eliminate IRI, the proposed strategy uses the inherent side information elimination mechanism in the NOMA-based CDRT system to eliminate the IRI of SR, and in turn uses SR technology to further improve the system capacity. The main contributions of this work can be summarized as follows:

1. We propose a novel 3−CDRT strategy. Compared to the HD and the FD cooperative NOMA strategies, the proposed strategy has obvious advantages. On the one hand, the SR technology can overcome the HD constrain and improve the spectral efficiency of FU. On the other hand, the transmission mechanism of CDRT enables relays to obtain side information for interference cancellation, thereby eliminating IRI;
2. We theoretically analyze the ergodic capacity of the near user (NU) and FU to evaluate the capacity performance of the proposed strategy. The derived results further show that the proposed strategy has the sum capacity scaling of $\log_2 \rho$ in the high ρ regime;

3. The simulation results show that the proposed strategy can increase the capacity of FU without affecting the capacity of NU, and enhance the sum capacity of the system compared with the other two benchmark strategies.

The rest of this paper is organized as follows. Section 2 describes the considered system model for 3−CDRT strategy. Then, we detail the relay's scheduling scheme and the transmission procedure of the 3−CDRT strategy in Section 3. In Section 4, the exact expression for the ergodic capacity of NU and FU is derived and the approximate ergodic capacity under high SNR is also derived. Simulation results are indicated in Section 5, followed by the conclusions in Section 6.

2. System Model

The system model of this paper is shown in Figure 1. Here we consider a multi-relay-based downlink NOMA transmission scenario, which includes a BS, a NU, N relay nodes $R_1, \cdots, R_N$, and a FU. The BS can communicate directly with the NU, but the direct communication link between the BS and the FU is unavailable due to the occlusion of the obstacle or the experience of deep fading. Therefore, the communication between the FU and the BS needs the help of the relay. In this paper, it is assumed that all nodes in the model are equipped with a single antenna, and all relay nodes work in HD and DF modes. Besides, it is assumed that all transmission channels experience independent but non-identically distributed (i.n.i.d) quasi-static Rayleigh fading channels, which means that the instantaneous channel gain of each channel remains constant in one transmit phase but varies between different phases. The channel coefficients from BS to NU, BS to relay R_i, and R_i to FU are, respectively, denoted as $h_{s,n}(t) \sim \mathcal{CN}(0, \lambda_{s,n})$, $h_{s,R_i}(t) \sim \mathcal{CN}(0, \lambda_{s,R_i})$, and $h_{R_i,f}(t) \sim \mathcal{CN}\left(0, \lambda_{R_i,f}\right)$, where $i \in \{1, 2, \cdots, N\}$. In addition, it is assumed that the statistical CSI of each channel is known at the corresponding node.

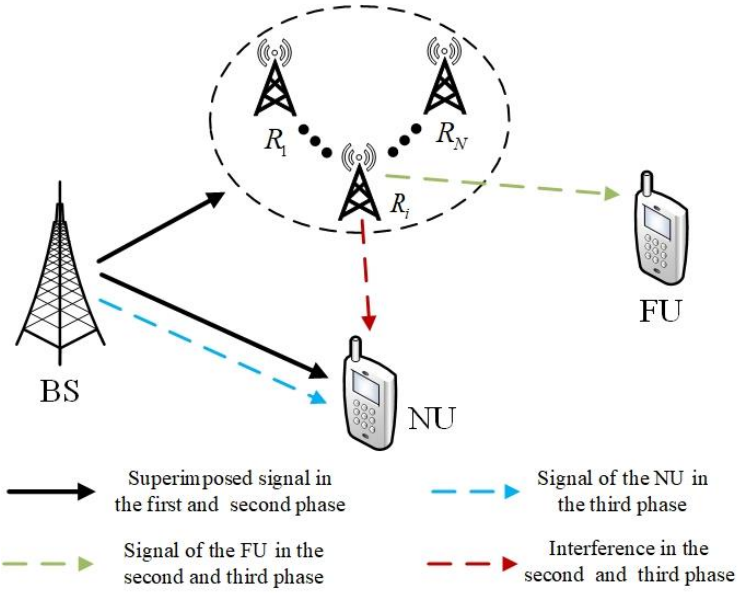


Figure 1. System model for 3−CDRT.

3. Three-Phase CDRT Strategy

In this section, we detail the proposed three-phase CDRT strategy. The proposed strategy is carried out in three phases.

(1) During the first phase, the BS transmits a superimposed signal $x_s(t_1) = \sqrt{\alpha P_s}\widetilde{x}_1 + \sqrt{\beta P_s}x_1$ where $\widetilde{x}_1$ and x_1 are the required signals from FU and NU with $E\left[|\widetilde{x}_1|^2\right] + E\left[|x_1|^2\right] = 1$. P_s is the transmit power of BS, and α and β are the power allocation

coefficients where $\alpha + \beta = 1$, $\alpha > \beta$. Thus, the received signals at NU and relays in the first phase can be expressed as:

$$y_n(t_1) = \sqrt{P_s}\left(\sqrt{\alpha}\widetilde{x}_1 + \sqrt{\beta}x_1\right)h_{s,n}(t_1) + n(t_1) \tag{1}$$

$$y_{R_k}(t_1) = \sqrt{P_s}\left(\sqrt{\alpha}\widetilde{x}_1 + \sqrt{\beta}x_1\right)h_{s,R_k}(t_1) + n_{R_k}(t_1), \forall R_k \in S \tag{2}$$

where $n(t_1)$ and $n_{R_k}(t_1)$ are the complex additive white Gaussian noise (AWGN) at NU and relay R_k, $S \triangleq \{R_1, R_2, \cdots, R_N\}$ is the initialized set of relay. According to the principle of successive interference cancelation (SIC), NU and R_k first treat x_1 as the interference and decode $\widetilde{x}_1$. Hence the SINR of $\widetilde{x}_1$ at NU and R_k can be derived as:

$$\widetilde{\gamma}_{s,n,1}(t_1) = \frac{\alpha\rho|h_{s,n}(t_1)|^2}{\beta\rho|h_{s,n}(t_1)|^2 + 1} \tag{3}$$

$$\widetilde{\gamma}_{s,R_k,1}(t_1) = \frac{\alpha\rho\left|h_{s,R_k}(t_1)\right|^2}{\beta\rho\left|h_{s,R_k}(t_1)\right|^2 + 1}, \forall R_k \in S \tag{4}$$

where $\rho \triangleq \frac{P_s}{\sigma^2}$ represents the transmit SNR. After decoding $\widetilde{x}_1$, NU remove $\widetilde{x}_1$ from the superimposed signal. It is assumed that all nodes can use SIC to perfectly cancellate the interference signal. Thus, when NU decode its own signal, the SNR can be given as:

$$\gamma_{s,n,1}(t_1) = \beta\rho|h_{s,n}(t_1)|^2 \tag{5}$$

and the instantaneous date rate of NU in the first phase can be derived as:

$$C_{x_1} \triangleq \frac{1}{3}\log_2(1 + \gamma_{s,n,1}(t_1)) \tag{6}$$

(2) During the second phase, one of the relays denoted R_1^* is first selected to forward $\widetilde{x}_1$. Since it is assumed that the nodes in the system only know the statistical CSI of the corresponding channel, the scheduling criterion of R_1^* can be defined as:

$$R_1^* \triangleq \text{argmax}_{r \in S}\text{min}\left\{\lambda_{s,r}, \lambda_{r,f}\right\} \tag{7}$$

According to the assumed system, there is no direct link between the BS and FU. Therefore, FU can only receive the signal from R_1^*, and the received signal at FU can be expressed as:

$$y_f(t_2) = \sqrt{P_r}h_{R_1^*,f}(t_2)\widetilde{x}_1 + n_f(t_2) \tag{8}$$

where P_r is the transmit power of R_1^* and $P_r = \mu P_s$, $0 < \mu \leq 1$, $y_f(t_2) = \sqrt{P_r}h_{R_1^*,f}(t_2)\widetilde{x}_1 + n_f(t_2)$ represents the AWGN at FU. The SNR of $\widetilde{x}_1$ at FU is given by

$$\widetilde{\gamma}_{R_1^*,f,1}(t_2) = \rho_r\left|h_{R_1^*,f}(t_2)\right|^2 \tag{9}$$

where $\rho_r = \frac{P_r}{\sigma^2}$.

Since the signal required by FU needs a two-hop link for transmission, the hop with the worst channel condition in the two-hop link determines the achievable rate of the FU. In addition, in order to ensure that the NU can cancellate the interference signal from the relay, the SINR at NU in the first phase also needs to be considered. Thus, according to (3), (4) and (9), the instantaneous date rate of FU in the second phase can be derived as:

$$C_{\widetilde{x}_1} \triangleq \frac{1}{3}\log_2\left\{1 + \text{min}\left\{\widetilde{\gamma}_{s,n,1}(t_1), \widetilde{\gamma}_{s,R_1^*,1}(t_1), \widetilde{\gamma}_{R_1^*,f,1}(t_2)\right\}\right\} \tag{10}$$

Simultaneously, the BS transmits a new superimposed signal $x_s(t_2) = \sqrt{\alpha P_s}\widetilde{x}_2 + \sqrt{\beta P_s}x_2$, where $\widetilde{x}_2$ and x_2 are the required signals from FU and NU in the second phase. The signals received by NU and the relay in the set $S\backslash R_1^*$ can be expressed as:

$$y_n(t_2) = \sqrt{P_s}\left(\sqrt{\alpha}\widetilde{x}_2 + \sqrt{\beta}x_2\right)h_{s,n}(t_2) + \sqrt{P_r}h_{R_1^*,n}(t_2)\widetilde{x}_1 + n(t_2) \tag{11}$$

$$y_{R_k}(t_2) = \sqrt{P_s}\left(\sqrt{\alpha}\widetilde{x}_2 + \sqrt{\beta}x_2\right)h_{s,R_k}(t_2) + \sqrt{P_r}h_{R_1^*,R_k}(t_2)\widetilde{x}_1 + n_{R_k}(t_2) \tag{12}$$

where $\forall R_k \in S\backslash R_1^*$ represents the relays in the set S except R_1^*. Since the relays in the set $S\backslash R_1^*$ and NU have decoded the signal $\widetilde{x}_1$ in the first phase, the interference signal $\sqrt{P_r}h_{R_1^*,R_k}(t_2)\widetilde{x}_1$ can be removed by applying SIC.

Then, similar to the first phase, only the superimposed signal from the BS remains in the received signal. According to the principle of NOMA, the relays in the set $S\backslash R_1^*$ and NU first treat x_2 as the interference and decode $\widetilde{x}_2$ and the SINR of $\widetilde{x}_2$ at NU and the relays in the set $S\backslash R_1^*$ can be derived as:

$$\widetilde{\gamma}_{s,n,2}(t_2) = \frac{\alpha\rho|h_{s,n}(t_2)|^2}{\beta\rho|h_{s,n}(t_2)|^2 + 1} \tag{13}$$

$$\widetilde{\gamma}_{s,R_k,2}(t_2) = \frac{\alpha\rho\left|h_{s,R_k}(t_2)\right|^2}{\beta\rho\left|h_{s,R_k}(t_2)\right|^2 + 1}, \forall R_k \in S\backslash R_1^* \tag{14}$$

After the NU decodes $\widetilde{x}_2$, it applies SIC to remove $\widetilde{x}_2$ from the superimposed signal sent by the BS again, and then decodes its own signal x_2, so the corresponding SNR is:

$$\gamma_{s,n,2}(t_2) = \beta\rho|h_{s,n}(t_2)|^2 \tag{15}$$

The instantaneous date rate of NU in the second phase can be derived as:

$$C_{x_2} \triangleq \frac{1}{3}\log_2(1 + \gamma_{s,n,2}(t_2)) \tag{16}$$

(3) During the third phase, similar to the second phase, one of the relay R_2^* is selected to forward $\widetilde{x}_2$ and the scheduling criterion of R_2^* can be defined as:

$$R_2^* \triangleq \arg\max_{r\in S\backslash R_1^*}\min\left\{\lambda_{s,r}, \lambda_{r,f}\right\} \tag{17}$$

and the received signal at FU can be expressed as:

$$y_f(t_3) = \sqrt{P_r}h_{R_2^*,f}(t_3)\widetilde{x}_2 + n_f(t_3) \tag{18}$$

Correspondingly, the SNR of $\widetilde{x}_1$ at FU is given by

$$\widetilde{\gamma}_{R_2^*,f,2}(t_3) = \rho_r\left|h_{R_2^*,f}(t_3)\right|^2 \tag{19}$$

Similarly, according to (13), (14) and (19), the instantaneous date rate of FU in the third phase can be derived as:

$$C_{\widetilde{x}_2} \triangleq \frac{1}{3}\log_2\left\{1 + \min\left\{\widetilde{\gamma}_{s,n,2}(t_2), \widetilde{\gamma}_{s,R_2^*,2}(t_2), \widetilde{\gamma}_{R_2^*,f,2}(t_3)\right\}\right\} \tag{20}$$

Simultaneously, the BS transmits a single signal $x_s(t_3) = \sqrt{\beta P_s}x_3$, where x_3 is the required signal from NU in the third phase. Thus, the signal received by NU can be expressed as:

$$y_n(t_3) = \sqrt{\beta P_s}h_{s,n}(t_3)x_3 + \sqrt{P_r}h_{R_2^*,n}(t_3)\widetilde{x}_2 + n(t_3) \tag{21}$$

Since NU have decoded the signal $\widetilde{x}_2$ in the second phase, the interference signal $\sqrt{P_r}h_{R_2^*,n}(t_3)\widetilde{x}_2$ can be removed by applying SIC and the SNR of x_3 at NU is expressed by

$$\gamma_{s,n,3}(t_3) = \beta\rho|h_{s,n}(t_3)|^2 \tag{22}$$

4. Capacity Analysis

When target data rate is determined by the channel conditions, the ergodic capacity is an important metric for performance evaluation. Thus, in this section, the ergodic capacity of NU and FU and the ergodic sum capacity are investigated.

4.1. Ergodic Capacity of NU

For the reason that the channel condition between BS and NU varies in different phase, but remains constant in one phase, the ergodic capacity of NU can be expressed as:

$$\overline{C}_N \triangleq E[C_{x_1}] + E[C_{x_2}] + E[C_{x_3}] = \overline{C}_{x_1} + \overline{C}_{x_2} + \overline{C}_{x_3} \tag{23}$$

where $E[\cdot]$ denotes the expectation operator.

In order to get the ergodic capacity of x_1, x_2, and x_3, let

$$X_i \triangleq \gamma_{s,n,i}(t_i) = \beta\rho|h_{s,n}(t_i)|^2, i \in \{1,2,3\} \tag{24}$$

X_i, $i \in \{1,2,3\}$ obey the exponential distribution, so the cumulative distribution functions (CDF) of X_i, $i \in \{1,2,3\}$ can be obtained as:

$$F_{X_i}(x_i) = 1 - e^{-\frac{x_i}{\beta\rho\lambda_{s,n}}}, i \in \{1,2,3\} \tag{25}$$

According to (6), the ergodic capacity of x_1 in the first phase can be expressed as:

$$\begin{aligned} \overline{C}_{x_1} &= E\left[\tfrac{1}{3}\log_2(1+\gamma_{s,n,1}(t_1))\right] = \tfrac{1}{3}\int_0^\infty \log_2(1+x) f_{X_1}(x)dx \\ &= -\tfrac{1}{3}\int_0^\infty \log_2(1+x)d\big(1-F_{X_1}(x)\big) = \tfrac{1}{3\ln 2}\int_0^\infty \tfrac{1-F_{X_1}(x)}{1+x}dx \end{aligned} \tag{26}$$

By using $\int_0^\infty \frac{e^{-\mu x}dx}{x+\beta} = -e^{\beta\mu}\mathrm{Ei}(-\mu\beta)$ [18] (eq.(3.352.4)), the closed expression for the ergodic capacity of x_1 in the first phase can be further expressed as:

$$\overline{C}_{x_1} = \frac{1}{3\ln 2}\int_0^\infty (1+x)^{-1} e^{-\frac{x}{\beta\rho\lambda_{s,n}}}dx = -\frac{1}{3\ln 2} e^{\frac{1}{\beta\rho\lambda_{s,n}}}\mathrm{Ei}\left(-\frac{1}{\beta\rho\lambda_{s,n}}\right) \tag{27}$$

Since the position of the NU in three phases does not change, the statistical characteristics of the channel condition will not change. Thus, the ergodic capacity of NU in each phase remains the same and the ergodic sum capacity of NU in three phases can be obtained as:

$$\overline{C}_N = \overline{C}_{x_1} + \overline{C}_{x_2} + \overline{C}_{x_3} = -\frac{1}{\ln 2} e^{\frac{1}{\beta\rho\lambda_{s,n}}}\mathrm{Ei}\left(-\frac{1}{\beta\rho\lambda_{s,n}}\right) \tag{28}$$

4.2. Ergodic Capacity of FU

Similarly, the ergodic capacity of FU can be expressed as:

$$\overline{C}_F \triangleq E\big(C_{\widetilde{x}_1}\big) + E\big(C_{\widetilde{x}_2}\big) = \overline{C}_{\widetilde{x}_1} + \overline{C}_{\widetilde{x}_2} \tag{29}$$

In order to solve the ergodic capacity of FU, we define

$$\begin{aligned} Y_i &\triangleq \min\left\{\widetilde{\gamma}_{s,n,i}(t_i), \widetilde{\gamma}_{s,R_i^*,i}(t_i), \widetilde{\gamma}_{R_i^*,f,i}(t_{i+1})\right\} \\ &= \min\left\{\frac{\alpha\rho|h_{s,n}(t_i)|^2}{\beta\rho|h_{s,n}(t_i)|^2+1}, \frac{\alpha\rho\left|h_{s,R_i^*}(t_i)\right|^2}{\beta\rho\left|h_{s,R_i^*}(t_i)\right|^2+1}, \rho_r\left|h_{R_i^*,f}(t_{i+1})\right|^2\right\}, i \in \{1,2\} \end{aligned} \tag{30}$$

In the high SNR regime, (30) can be approximated as:

$$Y_i = \min\left\{\frac{\alpha}{\beta}, \rho_r \left|h_{R_i^*,f}(t_{i+1})\right|^2\right\}, i \in \{1,2\} \tag{31}$$

Hence, the CDF of Y_i can be derived as:

$$\begin{aligned} F_{Y_i}(y) &= \Pr\left(\min\left(\tfrac{\alpha}{\beta}, \rho_r \left|h_{R_i^*,f}(t_{i+1})\right|^2\right) \le y\right) \\ &= 1 - \Pr\left(\min\left(\tfrac{\alpha}{\beta}, \rho_r \left|h_{R_i^*,f}(t_{i+1})\right|^2\right) > y\right) = \begin{cases} 1 - e^{-\frac{y}{\rho_r \lambda_{R_i^*,f}}} & y < \frac{\alpha}{\beta}, i \in \{1,2\} \\ 1 & y \ge \frac{\alpha}{\beta} \end{cases} \end{aligned} \tag{32}$$

By using $\int_u^v \frac{e^{-\mu x} dx}{x+\alpha} = e^{\alpha\mu}\{\mathrm{Ei}[-(\alpha+v)\mu] - \mathrm{Ei}[-(\alpha+u)\mu]\}$ [18] (eq.(3.352.3)), the closed expression for the ergodic capacity of $\widetilde{x}_i$, $i \in \{1,2\}$ can be further expressed as:

$$\begin{aligned} \overline{C}_{\widetilde{x}_i} &= \tfrac{1}{3}\int_0^\infty f_{Y_i}(y)\log_2(1+y)dy = \frac{1}{3\ln 2}\int_0^{\frac{\alpha}{\beta}} (1-y)^{-1} e^{-\frac{y}{\rho_r \lambda_{R_i^*,f}}} dy \\ &= \frac{1}{3\ln 2} e^{\frac{1}{\rho_r \lambda_{R_i^*,f}}} \left\{\mathrm{Ei}\left(-\left(1+\tfrac{\alpha}{\beta}\right)\frac{1}{\rho_r \lambda_{R_i^*,f}}\right) - \mathrm{Ei}\left(-\frac{1}{\rho_r \lambda_{R_i^*,f}}\right)\right\}, i \in \{1,2\} \end{aligned} \tag{33}$$

Thus, the ergodic capacity of FU can be derived as:

$$\begin{aligned} \overline{C}_F = &\tfrac{1}{3\ln 2} e^{\frac{1}{\rho_r \lambda_{R_1^*,f}}} \left\{\mathrm{Ei}\left(-\left(1+\tfrac{\alpha}{\beta}\right)\frac{1}{\rho_r \lambda_{R_1^*,f}}\right) - \mathrm{Ei}\left(-\frac{1}{\rho_r \lambda_{R_1^*,f}}\right)\right\} \\ &+ \tfrac{1}{3\ln 2} e^{\frac{1}{\rho_r \lambda_{R_2^*,f}}} \left\{\mathrm{Ei}\left(-\left(1+\tfrac{\alpha}{\beta}\right)\frac{1}{\rho_r \lambda_{R_2^*,f}}\right) - \mathrm{Ei}\left(-\frac{1}{\rho_r \lambda_{R_2^*,f}}\right)\right\} \end{aligned} \tag{34}$$

In traditional two-phase CDRT strategy (2−CDRT) [6], the ergodic capacity of FU is:

$$\overline{C}_F^{CDRT} = \frac{1}{2\ln 2} e^{\frac{1}{\rho_r \lambda_{r,f}}} \left\{\mathrm{Ei}\left(-\left(1+\frac{\alpha}{\beta}\right)\frac{1}{\beta\rho_r \lambda_{r,f}}\right) - \mathrm{Ei}\left(-\frac{1}{\rho_r \lambda_{r,f}}\right)\right\} \tag{35}$$

It can be seen that when $\lambda_{R_1^*,f} = \lambda_{R_2^*,f} = \lambda_{r,f}$, the proposed strategy will bring 4/3 times of gain to the ergodic capacity of FU compared with 2−CDRT strategy. In fact, since the compared 2−CDRT strategy uses the same relay scheduling scheme as the proposed strategy, statistically speaking, $\lambda_{R_1^*,f}, \lambda_{R_2^*,f}$, and $\lambda_{r,f}$ are very close in value. Therefore, the actual gain brought by the proposed strategy is indeed close to 4/3.

4.3. Ergodic Sum Capacity and Its Approximation

According to (28) and (33), the ergodic sum capacity can be expressed as:

$$\begin{aligned} \overline{C}_{\text{sum}} = &\overline{C}_{x_1} + \overline{C}_{x_2} + \overline{C}_{x_3} + \overline{C}_{\widetilde{x}_1} + \overline{C}_{\widetilde{x}_2} = -\tfrac{1}{\ln 2} e^{\frac{1}{\beta\rho\lambda_{s,n}}} \mathrm{Ei}\left(-\frac{1}{\beta\rho\lambda_{s,n}}\right) \\ &+ \tfrac{1}{3\ln 2} e^{\frac{1}{\rho_r \lambda_{R_1^*,f}}} \left\{\mathrm{Ei}\left(-\left(1+\tfrac{\alpha}{\beta}\right)\frac{1}{\rho_r \lambda_{R_1^*,f}}\right) - \mathrm{Ei}\left(-\frac{1}{\rho_r \lambda_{R_1^*,f}}\right)\right\} \\ &+ \tfrac{1}{3\ln 2} e^{\frac{1}{\rho_r \lambda_{R_2^*,f}}} \left\{\mathrm{Ei}\left(-\left(1+\tfrac{\alpha}{\beta}\right)\frac{1}{\rho_r \lambda_{R_2^*,f}}\right) - \mathrm{Ei}\left(-\frac{1}{\rho_r \lambda_{R_2^*,f}}\right)\right\} \end{aligned} \tag{36}$$

Theorem 1. When ρ, $\rho_r \to \infty$ the scaling of $\overline{C}_{sum}$ is $\log_2 \rho$.

Proof of Theorem 1. In high SNR regime, by employing the approximations of $\lim_{x\to 0} e^{-x} \sim 1 - x$ and $\lim_{x\to 0} \mathrm{Ei}(x) \sim C + \ln(-x) + x$, where C denotes the Euler constant, the approximation of $\overline{C}_N$ can be derived as:

$$\overline{C}_N \sim -\frac{1}{\ln 2}\left(1 + \frac{1}{\beta\rho\lambda_{s,n}}\right)\left(C + \ln\left(\frac{1}{\beta\rho\lambda_{s,n}}\right) - \frac{1}{\beta\rho\lambda_{s,n}}\right) \sim \log_2 \rho \tag{37}$$

Similarly, it can be deduced that the approximate ergodic capacity of FU under high SNR is

$$\begin{aligned}\overline{C}_F \sim \frac{1}{3\ln 2}\Bigg\{&\left(1+\frac{1}{\rho_r\lambda_{R_1^*,f}}\right)\left[C_1+\ln\left(\frac{1}{\beta\rho_r\lambda_{R_1^*,f}}\right)-\frac{1}{\beta\rho_r\lambda_{R_1^*,f}}-C_2\right.\\&\left.-\ln\left(\frac{1}{\rho_r\lambda_{R_1^*,f}}\right)+\frac{1}{\rho_r\lambda_{R_1^*,f}}\right]+\left(1+\frac{1}{\rho_r\lambda_{R_2^*,f}}\right)\left[C_3+\ln\left(\frac{1}{\beta\rho_r\lambda_{R_2^*,f}}\right)\right.\\&\left.-\frac{1}{\beta\rho_r\lambda_{R_2^*,f}}-C_4-\ln\left(\frac{1}{\rho_r\lambda_{R_2^*,f}}\right)+\frac{1}{\rho_r\lambda_{R_2^*,f}}\right]\Bigg\}\sim\frac{2}{3}\log_2\left(\frac{1}{\beta}\right)\end{aligned} \tag{38}$$

According to (37) and (38), it can be observed that in high SNR regime, the scaling of $\overline{C}_N$ and $\overline{C}_F$ are $\log_2\rho$ and $\frac{2}{3}\log_2\left(\frac{1}{\beta}\right)$ respectively. Thus, the approximate ergodic sum capacity can be given by

$$\overline{C}_{sum} \sim \log_2\rho \tag{39}$$

□

4.4. Benchmark Strategies

In this subsection, in order to further study the advantages of the proposed strategy, we use the following two benchmark strategies as a comparison.

1. Traditional two-phase CDRT strategy (2−CDRT) [6]: The 2−CDRT strategy is carried out within two phases. During the first phase, the BS broadcasts the superimposed signal of the signals required by NU and FU, and allocates more power to the signal required by FU. Meanwhile, a relay is scheduled to decode the signal of FU. During the second phase, the BS only broadcasts a new signal that required by NU and the scheduled relay forwards the signal that required by FU in the first phase. By a derivation similar to the work above, the ergodic sum capacity of the 2−CDRT strategy can be given by

$$\begin{aligned}&\overline{C}_{\mathrm{CDRT}}\\&=-\frac{1}{\ln 2}e^{\frac{1}{\beta\rho\lambda_{s,n}}}\mathrm{Ei}\left(-\frac{1}{\beta\rho\lambda_{s,n}}\right)+\frac{1}{2\ln 2}e^{\frac{1}{\rho r\lambda_{r,f}}}\left\{\mathrm{Ei}\left(-\left(1+\frac{\alpha}{\beta}\right)\frac{1}{\beta\rho_r\lambda_{r,f}}\right)-\mathrm{Ei}\left(-\frac{1}{\rho_r\lambda_{r,f}}\right)\right\}\end{aligned} \tag{40}$$

2. OMA-based 3−CDRT strategy (3−CDRT−OMA): Compared with the strategy proposed in this paper, the 3−CDRT−OMA strategy needs to divide more phases to complete because only a single signal transmission is allowed in each phase. Specifically, the transmission process is divided into 7 phases in the 3−CDRT−OMA strategy. Thus, the ergodic sum capacity of the 3−CDRT−OMA strategy can be expressed as:

$$\begin{aligned}\overline{C}_{\mathrm{OMA}}=&-\frac{3e^{\frac{1}{\rho\lambda_{s,n}}}}{7\ln 2}\mathrm{Ei}\left(-\frac{1}{\rho\lambda_{s,n}}\right)-\frac{e^{\left(\frac{1}{\rho\lambda_{s,R_1}}+\frac{1}{\rho_r\lambda_{R_1,f}}\right)}}{7\ln 2}\mathrm{Ei}\left(-\frac{1}{\rho\lambda_{s,R_1}}-\frac{1}{\rho_r\lambda_{R_1,f}}\right)\\&-\frac{e^{\left(\frac{1}{\rho\lambda_{s,R_2}}+\frac{1}{\rho_r\lambda_{R_2,f}}\right)}}{7\ln 2}\mathrm{Ei}\left(-\frac{1}{\rho\lambda_{s,R_2}}-\frac{1}{\rho_r\lambda_{R_2,f}}\right)\end{aligned} \tag{41}$$

5. Simulation Result

In this section, we present simulations to verify the theoretical results and demonstrate the advantages of the proposed strategy. Without loss of generality, we consider the scenario where the BS locates at coordinate (0,0) and all relays randomly locate within a circle centered at coordinate (50 m,0) and with a radius being 20 m. The distances between the BS and NU and FU are set to 45 m and 100 m respectively and the power allocation coefficients are set as $\alpha = 0.9$, $\beta = 0.1$. In our simulation, we set $\mu = 1$ which is reasonable according to the LTE standards in [19]. Furthermore, the noise power is set to $\sigma^2 = -60$ dBm, and the path loss attenuation is modeled as $\lambda_{a,b} \triangleq 1/\left[1+(d/d_0)^v\right]$, where $d_{a,b}$ denotes the distance between the node a and node b, $d_0 = 20$ denotes the reference distance, and $v = 2.7$ denotes the path loss exponent.

In Figure 2, the proposed 3−CDRT strategy is compared with the 2−CDRT and the 3−CDRT−OMA strategies in terms of the ergodic sum capacity. First, it can be observed that the analytical results and the simulated results precisely match, which proves the correctness of the analysis results. The figure also verifies the result of Theorem 1 that $\overline{C}_{sum}$ has the scaling of $\log_2 \rho$. Furthermore, it can be seen that the proposed strategy outperforms the other two strategies. In terms of the ergodic sum capacity, the 3−CDRT−OMA strategy is far inferior to the proposed strategy. The 2−CDRT has the same slope as the proposed strategy, but with the same P_s, the proposed strategy can bring an ergodic capacity gain of about 0.5 bps/Hz. Conversely, to achieve the same ergodic sum capacity, the P_s of 2−CDRT needs to be about 2 dBm higher than the proposed strategy, which shows that the proposed strategy can help the smart grid achieve higher system capacity with less energy consumption. The reason is that compared with the 2−CDRT and the 3−CDRT−OMA strategies, the proposed strategy can transmit more signals per phase on average due to the adoption of NOMA technology and SR technology.

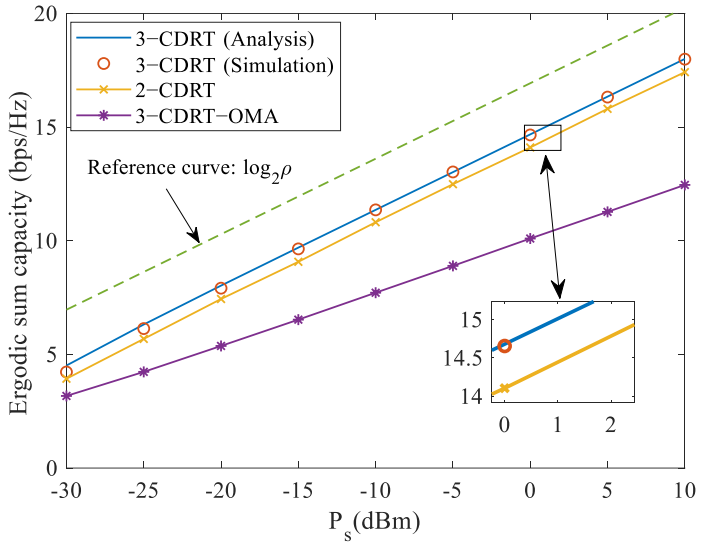


Figure 2. Comparison among the proposed 3−CDRT strategy, the 2−CDRT strategy and the 3−CDRT−OMA strategy in terms of the ergodic sum capacity with varying P_s(dBm).

Figure 3 shows the ergodic capacity of NU achieved by the proposed strategy, the 2−CDRT strategy, and the 3−CDRT−OMA strategy with varying P_s. From the figure we can find that the analytical results and the simulated results precisely match, and the scales of $\overline{C}_N$ is $\log_2 \rho$. Besides, it can be observed that the proposed strategy and the 2−CDRT strategy achieve approximately the same ergodic capacity of NU. Because in these two strategies, the BS both transmits the signals of NU in all the phases. In addition, the curve of $\overline{C}_N$ under the proposed strategy performs batter than that of the 3−CDRT−OMA strategy in both numerical value and growth rate. This is because the OMA transmission method is adopted in the 3−CDRT−OMA strategy, which results in that only one signal can be transmitted by one node in each phase, thus reducing the spectrum efficiency of the NU. Furthermore, it can be observed that the decrease of the distance between the BS and NU can lead to an increase of $\overline{C}_N$.

Figure 4 shows the ergodic capacity of FU achieved by the proposed strategy, the 2−CDRT strategy, and the 3−CDRT−OMA strategy with varying P_s. In medium and high SNR regime, the analysis results precisely match the simulated results. But due to the high SNR approximation when processing $\overline{C}_F$, there is a small mismatch between the analysis and simulated results in the low power regime. Besides, it can be seen that $\overline{C}_F$ under the 3−CDRT strategy is higher than that of the 2−CDRT strategy, Since the 3−CDRT strategy transmits more signals of FU per phase on average.

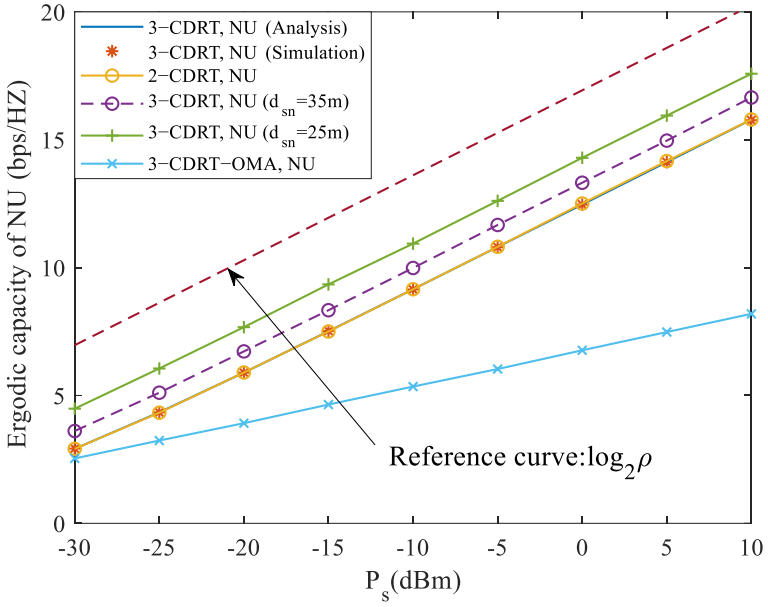


Figure 3. Comparison among the proposed 3−CDRT strategy, the 2−CDRT strategy and the 3−CDRT−OMA strategy in terms of the ergodic capacity of NU with varying P_s(dBm).

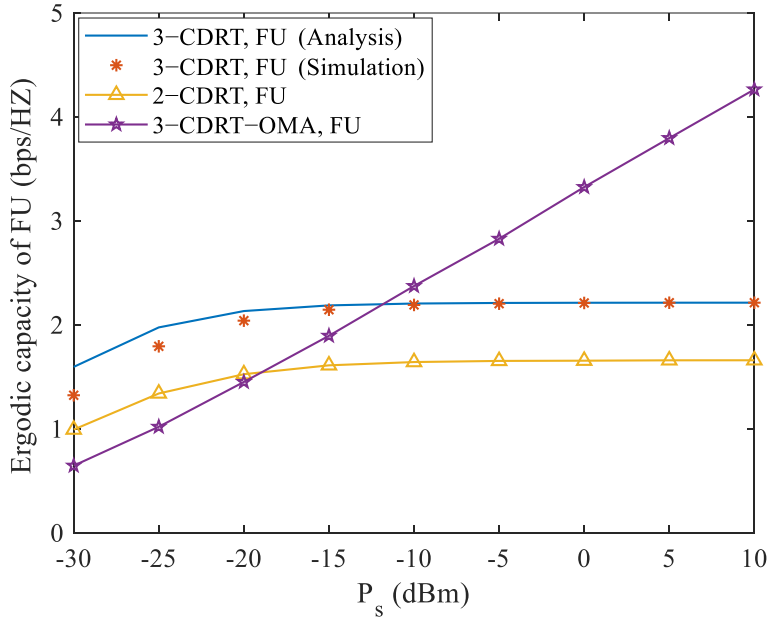


Figure 4. Comparison among the proposed 3−CDRT strategy, the 2−CDRT strategy and the 3−CDRT−OMA strategy in terms of the ergodic capacity of FU with varying P_s(dBm).

Meanwhile, we can see that with the increase of P_s, $\overline{C}_F$ under the 2−CDRT and 3−CDRT strategies increase first and then saturate, while $\overline{C}_F$ under the 3−CDRT−OMA strategy gradually increases. This observation can be intuitively explained as follows. According to (10), the hop with the worst channel condition in the two-hop link determines the achievable rate of the FU. In the 2−CDRT and 3−CDRT strategies, the scheduled relay needs to decode the FU's signal while regarding the NU's signal as interference. But in the 3−CDRT−OMA strategy, the FU's signals can be decoded without interference in both hops. Thus, $\overline{C}_F$ under the 3−CDRT−OMA strategy has better performance than that under the strategies based on NOMA in high power regime. But on the other hand, combining with Figures 2 and 3, it can be concluded that in the 3−CDRT−OMA strategy, the performance gain of $\overline{C}_F$ is obtained at the expense of the system capacity.

In order to analyze the impact of the proposed 3−CDRT strategy on power grid stability, we compare the outage probability of FU among the proposed 3−CDRT strategy, the 2−CDRT strategy and the 3−CDRT−OMA strategy in terms of the outage probability of FU with varying P_s in Figure 5. It can be observed that with the increase of P_s, the outage probability of each strategy decreases. Due to the low capacity of the far user channel in the 2−CDRT strategy, when the target rate of FU is 1.8, its outage probability is always 1. In addition, it can be observed that the 3−CDRT strategy has a lower far user outage probability than the 2−CDRT strategy because its higher capacity. Furthermore, similar to the analysis in Figure 4, the 3−CDRT−OMA strategy sacrifices the performance of NU thus has lower outage probability of NU in the high SNR regime. However, it can be seen that the proposed strategy is much better than the 3−CDRT−OMA strategy in the middle and low power regimes. Therefore, from the perspective of energy consumption, the proposed strategy is more suitable for achieving stable communication of FU with low power consumption.

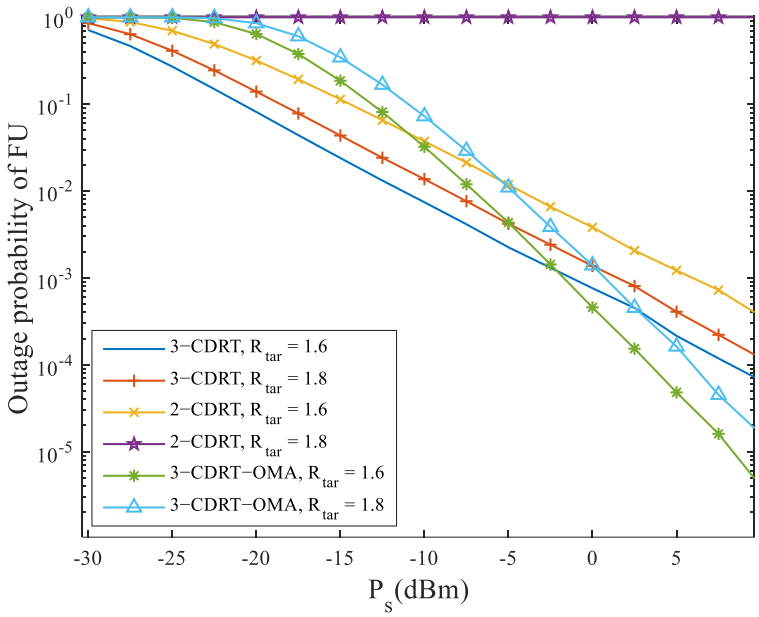


Figure 5. Comparison among the proposed 3−CDRT strategy, the 2−CDRT strategy and the 3−CDRT−OMA strategy in terms of the outage probability of FU with varying P_s(dBm).

We further compare the impact of the proposed strategy with the other two benchmark strategies on the transmission delay with varying P_s in Figure 6. First, it can be observed that with the increase of P_s, the transmission delay of each strategy decreases. Besides, in terms of the transmission delay of NU, the proposed 3−CDRT strategy and the 2−CDRT strategy have basically the same performance because they have the same ergodic capacity of NU, while the 3−CDRT−OMA strategy is inferior to the other two strategies. In terms of transmission delay of FU, the proposed 3−CDRT strategy is far superior to the 2−CDRT strategy in all power regimes and is superior to the 3−CDRT−OMA strategy in the middle and low power regimes. Combined with the transmission delay performance of NU, it can be found that in the 3−CDRT−OMA strategy, the performance gain of the transmission delay of FU in high power regime is obtained at the expense of the transmission delay of NU.

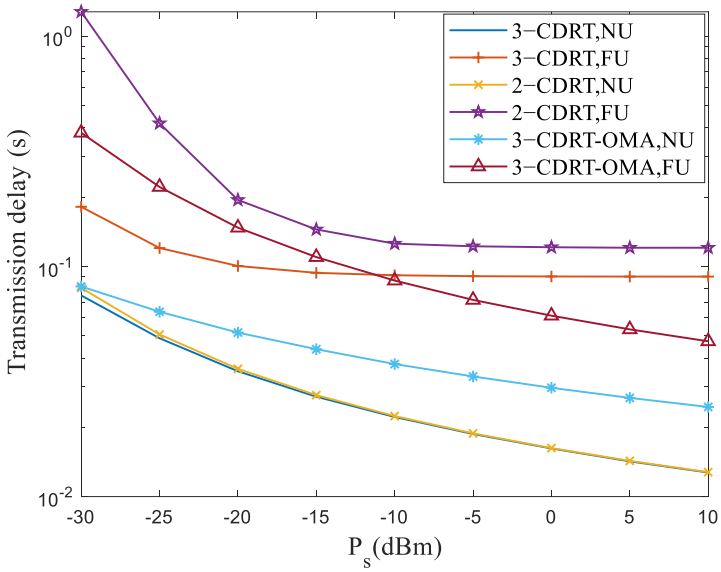


Figure 6. Comparison among the proposed 3−CDRT strategy, the 2−CDRT strategy and the 3−CDRT−OMA strategy in terms of the transmission delay with varying P_s(dBm).

6. Conclusions

In this paper, we propose a new 3−CDRT strategy based on SR to improve the capacity of smart grid. The proposed study utilizes SR technology to virtual FD relay to improve the spectral efficiency of FU without affecting the capacity of NU. Besides, the proposed strategy can eliminate the IRI through the transmission mechanism of CDRT. To further evaluate the performance of the proposed strategy, we derived the exact expression for the ergodic capacity of the NU and FU and also carried out the approximate ergodic capacity under high SNR. Theoretical analysis shows that the proposed strategy can allow the system transmits more signals of FU per phase on average which improves the ergodic capacity of FU. At last, simulation results were presented to verify the accuracy of the theoretical results and demonstrate the advantage of the proposed strategy.

Author Contributions: Conceptualization, J.S. and M.L.; methodology, J.S.; software, J.S.; validation, G.L., J.R., L.Y. and Y.L.; formal analysis, Y.Z.; investigation, J.C.; resources, G.L., J.R., L.Y. and Y.L.; data curation, M.L.; writing—original draft preparation, M.L.; writing—review and editing, Y.Z.; visualization, M.L.; supervision, Y.Z. and J.C.; project administration, J.C.; funding acquisition, J.R. All authors have read and agreed to the published version of the manuscript.

Funding: This work is jointly supported by the Laboratory Open Fund of Beijing Smart-chip Microelectronics Technology Co., Ltd., and the National Natural Science Foundation of China (No. 61901312).

Conflicts of Interest: The authors declare no conflict of interest.

References

1. Gong, G.; Sun, Y.; Cai, M. Research of network architecture and implementing scheme for the internet of things towards the smart grid. *Power Syst. Prot. Control* **2011**, *39*, 52–58.
2. Dai, L.; Wang, B.; Ding, Z.; Wang, Z.; Chen, S.; Hanzo, L. A survey of non-orthogonal multiple access for 5G. *IEEE Commun. Surv. Tutor.* **2018**, *20*, 2294–2323. [CrossRef]
3. Liu, C.; Liang, D. Heterogeneous Networks with Power-Domain NOMA: Coverage, Throughput, and Power Allocation Analysis. *IEEE Trans. Wirel. Commun.* **2018**, *17*, 3524–3539. [CrossRef]
4. Lu, H.; Shu, F.; Min, L.; Wang, Y. Abstract Structure of Data Communication in IoT Application. In Proceedings of the 2018 IEEE 4th International Conference on Computer and Communications (ICCC), Chengdu, China, 7–10 December 2018; pp. 829–834.
5. Laneman, J.N.; Tse, D.N.C.; Wornell, G.W. Cooperative diversity in wireless networks: Efficient protocols and outage behavior. *IEEE Trans. Inf. Theory* **2004**, *50*, 3062–3080. [CrossRef]
6. Kim, J.; Lee, I. Non-Orthogonal Multiple Access in Coordinated Direct and Relay Transmission. *IEEE Commun. Lett.* **2015**, *19*, 2037–2040. [CrossRef]

7. Yang, M.; Chen, J.; Hu, R.Q.; Yang, L. Non-Orthogonal Multiple Access with Cooperative Direct and User-Assisted Transmission. *IEEE Commun. Lett.* **2021**, *25*, 264–268. [CrossRef]
8. Xu, Y.; Wang, G.; Zheng, L.; Jia, S. Performance of NOMA-based coordinated direct and relay transmission using dynamic scheme. *IET Commun.* **2018**, *12*, 2231–2242. [CrossRef]
9. Zhong, C.; Zhang, Z. Non-Orthogonal Multiple Access with Cooperative Full-Duplex Relaying. *IEEE Commun. Lett.* **2016**, *20*, 2478–2481. [CrossRef]
10. Yang, S.; Belfiore, J.-C. Towards the Optimal Amplify-And-Forward Cooperative Diversity Scheme. *IEEE Trans. Inf. Theory* **2007**, *53*, 3114–3126. [CrossRef]
11. Tannious, R.; Nosratinia, A. Spectrally-Efficient Relay Selection with Limited Feedback. *IEEE J. Sel. Areas Commun.* **2008**, *26*, 1419–1428. [CrossRef]
12. Rankov, B.; Wittneben, A. Spectral Efficient Protocols for Half-Duplex Fading Relay Channels. *IEEE J. Sel. Areas Commun.* **2007**, *25*, 379–389. [CrossRef]
13. Liau, Q.Y.; Leow, C.Y.; Ding, Z. Amplify-and-Forward Virtual Full-Duplex Relaying-Based Cooperative NOMA. *IEEE Wirel. Commun. Lett.* **2018**, *7*, 464–467. [CrossRef]
14. Fan, Y.; Wang, C.; Thompson, J.; Poor, H.V. Recovering Multiplexing Loss through Successive Relaying Using Repetition Coding. *IEEE Trans. Wirel. Commun.* **2007**, *6*, 4484–4493. [CrossRef]
15. Wei, J.; Wei, J.; Hu, S.; Chen, W. Successive Decode-and-Forward Relaying With Privacy-Aware Interference Suppression. *IEEE Access* **2020**, *8*, 95793–95806. [CrossRef]
16. Ji, Y.; Han, C.; Wang, A. Partial inter-relay interference cancellation in two path successive relay network. *IEEE Commun. Lett.* **2014**, *18*, 451–454. [CrossRef]
17. Deng, R.; Dou, G.; Gao, J.; Wang, Q. The Interference Cancellation Scheme for AF Successive Relay Networks Based on Postmultiplying Precoding. In Proceedings of the 2018 14th International Conference on Natural Computation, Fuzzy Systems and Knowledge Discovery (ICNC-FSKD), Huangshan, China, 28–30 July 2018; pp. 1289–1293.
18. Gradshteyn, I.S.; Ryzhik, I.M. *Table of Integrals, Series, and Products*, 7th ed.; Academic Press: Amsterdam, The Netherlands, 2007.
19. *LTE; Evolved Universal Terrestrial Radio Access (E-UTRA); Base Station (BS) Radio Transmission and Reception*; International Telecommunication Union: Geneva, Switzerland, 2014.